Geomechanik 5/2008: ☐ druckfrei ☐ nach Korrektur druckfrei
Nr. 056

Datum, Unterschrift

Topics

DOI: 10.1002/geot.200800056

Nedim Radoncic
Karl Großauer
Wulf Schubert
Hans-Jörg Gober
Günther Heigerth

Improved Design Method for Pre-stressed Water Tunnels

The final design of the pumped-storage project Feldsee features a complex lining and pre-stress grouting concept, rendering the method presented by *Seeber* insufficient for an accurate determination of the system behaviour in all stages of construction and operation. A calculation procedure based on the matrix stiffness method has been implemented, allowing incorporation of multi-stage pre-stressing injections at different locations of a lining being composed of several layers with different mechanical properties. Based on the design obtained by applying the above method, another question of maximum allowable non-symmetric displacement of the pre-cast concrete segment arose. A parametric study has been used to determine the boundaries of asymmetric displacements throughout the pre-stressing procedure, allowing establishment of threshold values for the monitoring conducted during the pre-stressing injections.

Fortschrittliche Bemessungsverfahren für vorgespannte Wassertunnel

Der endgültige Entwurf des Pumpspeicherkraftwerkes Feldsee weist ein komplexes Auskleidungs- und Injektionskonzept auf, bei dem die Rechenmethode nach Seeber keine adäquate Vorhersage des Systemverhaltens in allen Bau- und Betriebszuständen erlaubt. Ein auf der Deformationsmethode basierendes Rechenverfahren wurde angewandt, um die Einflüsse von mehrstufigen Vorspanninjektionen und einer Auskleidung, die aus mehreren Schichten mit unterschiedlichen mechanischen Eigenschaften besteht, zu erfassen. Aus den Ergebnissen dieser Rechenmethode ergab sich die weitere Frage nach der maximal zulässigen Ovalität des Beton-Fertigteilrohrs. Eine Parameterstudie wurde durchgeführt, um die Ovalität der Auskleidung zu ermitteln. Sie wird zur Aufstellung von Warnwerten für die während der Vorspanninjektionen gemessenen Verschiebungen herangezogen.

1 Introduction

The Feldsee pressure tunnel is the newest pumped-storage extension to the KELAG's group of Fragrant hydropower stations. It connects two existing reservoirs, Feldsee at 2,200 m a.s.l. and Wurten at 1,700 m a.s.l. in a daily operated pump storage scheme with a peak output of 70 MW. The pressure conduit is composed of two parts: the vertical shaft, constructed by raise-boring technique, and the moderately inclined tunnel, excavated conventionally. The maximum pressure head in the conduit equals 820 m, dictated by rapid shutdown procedure of the turbine and the resulting additional dynamic loading amounting to 40 % of the hydrostatic pressure. The surrounding rock mass is mainly composed of massive, unweathered gneiss with

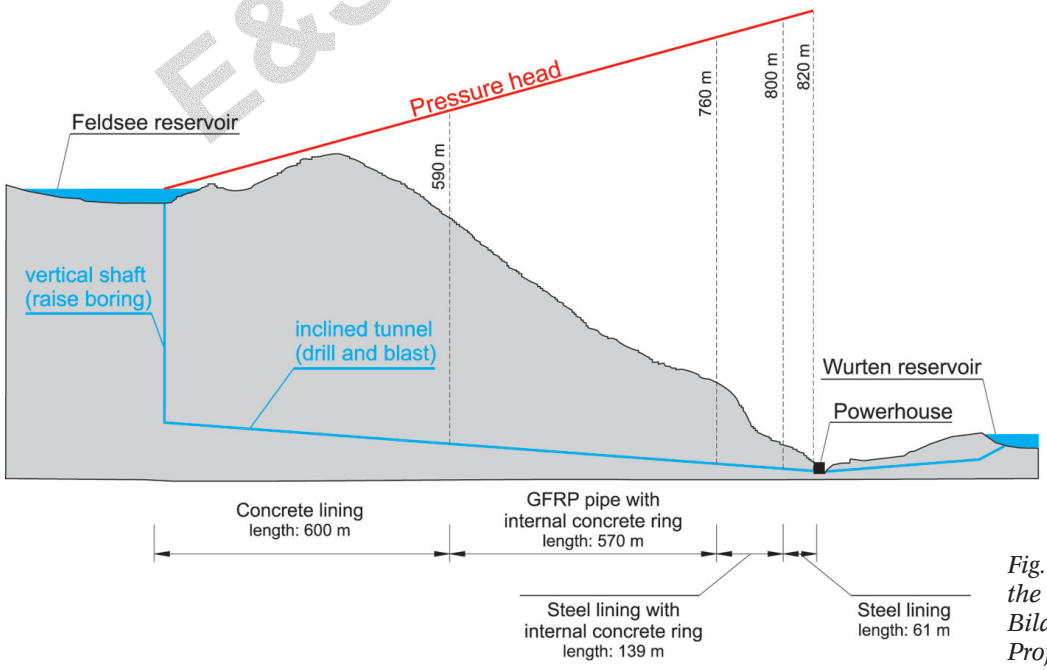

Fig. 1. Longitudinal section of the Feldsee project
Bild 1. Längsschnitt des Feldsee Projekts

widely spaced joints of low persistence. The high overburden grants good confinement for the internal pressure loading, hence resulting in perfect conditions for using external grout injections in order to pre-stress the inner concrete lining and utilize the load-bearing capacity of the ground as far as possible [1]. The final solution features pre-cast concrete segments with a thin steel lining in the lower part of the inclined tunnel, and pre-cast concrete segments with a "glass fibre reinforced polymer" (GFRP) lining in the upper part (Figure 1). The lowest part of the tunnel is made of steel lining without any utilization of the ground put into account, due to low overburden and more frequently jointed rock mass.

The design of the Feldsee pressure tunnel is based on principles and methods being state-of-the-art for a relatively long time. However, the usage of a GFRP pipe as water sealing element and the applied injection concept represent features requiring usage of calculation methods going beyond the ones introduced by *Seeber* [2]. The following aspects had to be accounted for in detail in order to obtain an economical and safe design:

a) The determination of the load-bearing capacity and the associated load-displacement relationship of the ground;
b) The issue of interaction between three different pre-stressing grout injections at two different positions of the lining, and the determination of the system behaviour at all stages;
c) The assessment of the temperature and creep losses, based on results of b);
d) Determination of maximum allowable unsymmetrical deformations, in order to avoid stress concentrations in the pre-cast concrete inner lining.

The contents of this case-study are concentrated on presenting the applied methods and their results.

2 Determination of rock mass properties

The general load-displacement behaviour under inner pressure loading and its contribution to the overall system stiffness represent one of the key design parameters. In order to verify the assumptions made in the initial design phase and refine the entire concept, an extensive testing programme has been conducted. The choice of the test locations for the large-scale plate load test aimed on establishing an envelope of the lowest expectable rock mass properties. Five cross sections have been selected, each of them featuring a rock mass quality relatively lower then the one encountered in the major part of the tunnel. On every test location, two plate load tests have been performed: one with the loading direction parallel to the foliation orientation and the other one perpendicular to it, addressing the rock mass anisotropy inherent to metamorphic rocks.

The displacements have been measured by utilizing a single magnetic extensometer aligned with the axis of the load plate. It monitored the displacement of four magnets which were stiffly bonded with the rock mass. On every side of the test jack frame, they were positioned at the depths of approximately 30, 50, 125 and 230 cm measured from the respective outward rim of the load plate (Figure 2). The results allowed a relative confirmation of the initial assessments of the rock mass deformability, while underlining the expected anisotropy of the rock mass.

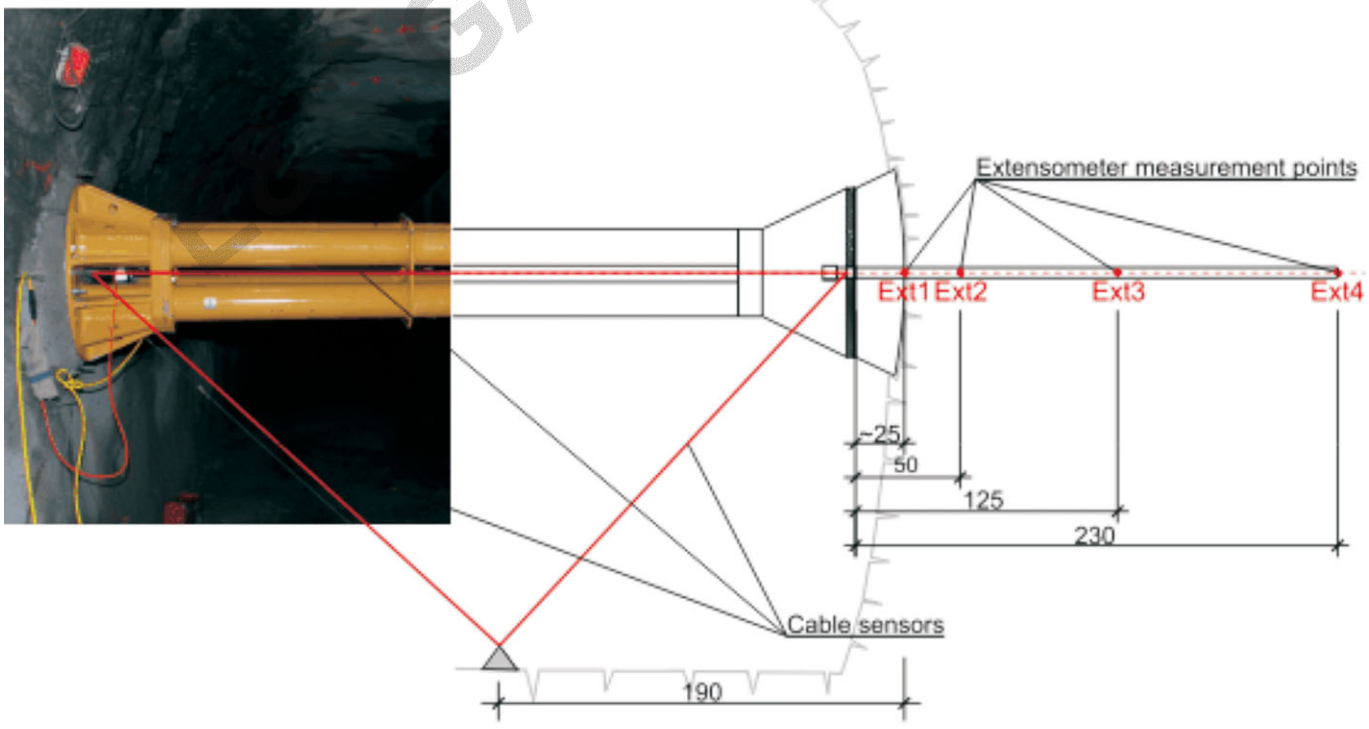

Fig. 2. Test geometry and the sensor set-up
Bild 2. Geometrie des Versuchsaufbaus und die Anordnung der Messgeber

The existence of the blasting damage zone has been confirmed as well, since the rock mass properties were severely reduced in the vicinity of the tunnel. The average deformation modulus in direction perpendicular to the foliation and calculated from the displacements of the load plate equalled 4,768 MPa, with the cross section at chainage 179 featuring extremely low 979 MPa. Luckily, the deeper positioned extensometers confirmed that the blasting damage zone is bounded to the vicinity of the tunnel, with the deformation moduli parallel to the foliation rising well above 10,000 MPa. The deformation moduli perpendicular to the foliation also featured acceptable values beyond 5,000 MPa.

After the elastic properties of the ground have been determined by the plate-load tests, particular attention had to be paid to the fact that the high internal pressure was likely to induce tensile cracks in the rock mass, perpendicular to the direction of the lowest principal stress. Due to the load level and the stress distribution induced by the plate load test, no information about the tensile strength of the ground could be derived from the test results. Numerical back analysis yielded highly plausible results [3] (with influences of tunnel geometry and test set-up incorporated as well), and underlined that the changes in the stress field caused by the plate-load test dissipate very quickly and are too small to induce any noticeable tensile failure in the rock mass.

At the beginning of the GFRP-lined part of the tunnel, the overburden of 163 m was deemed not high enough to result in full containment (and thus, purely elastic response) for the given magnitude of loading. The generation of tensile cracks results in a considerable flattening of the overall load-displacement curve of the rock mass (Figure 3).

The closed-form solutions allowing the calculation of the extent of the crack propagation and their influence on the load-displacement relationship have been presented by *Seeber* [2] and *Feder* [4]. The solution in [2] is fully applicable only in case of hydrostatic primary stress state, while the solution by *Feder* [4] represents an approximation.

Nevertheless, the load-displacement relationships (see Figure 3) thus obtained proved to match well with the data obtained from numerical simulations, and were used henceforth as good approximations. Additional reason for the usage of the closed-form solutions for the assessment of the tensile cracks is the underlying assumption of a concentric, circular crack zone around the tunnel. In reality, the deformations induced by excessive internal pressure concentrate on existing joints and are usually singular (there is no smeared cracking zone), while the rest of the rock mass retains a much stiffer load bearing characteristic, rendering the application of the closed-form solutions as "being on the safe side" in such cases.

3 General design of the GFRP-lined section

The section of the tunnel utilizing GFRP pipes as impermeable elements starts at station 198, with an overburden of 163 m. The good ground quality grants that despite relatively high stresses, no failure of the rock mass is expected after the excavation and the associated stress re-distribution. On the other hand, apart from the area with the moderate overburden at the beginning of the GFRP-lined tunnel segment, the high stresses grant good confinement to the internal pressure resulting from the grouting injections and water pressure. Hence, the concept was oriented towards maximal possible utilization of the ground, relying on the stiffness of the surrounding rock mass to limit the deformations of the lining to the amount where no tensile strains, and hence tensile stresses, occur. The cross section is composed of an outer concrete shell of lower strength (C25/35) cast on site. Prior to the casting of the shell, the tunnel walls have been sprayed with lime water, breaking the possible adhesive bond between the concrete and the rock mass and thus helping to obtain a balanced pressure distribution during pre-stressing. Three grouting conduits have been installed longitudinally, with a segment length of 16 m. After the construction of the tunnel was finished, pre-cast concrete segments (C40/50) with a

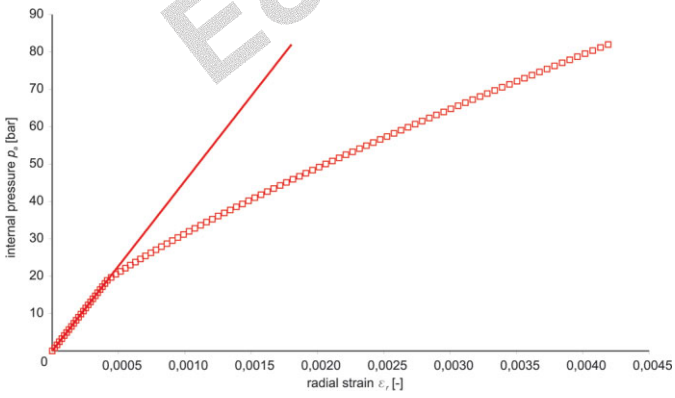

Fig. 3. Decrease of the overall rock mass stiffness due to development of tensile cracks (line: linear elastic behaviour, squares: the effect of brittle cracking)
Bild 3. Abnahme der globalen Steifigkeit des Gebirges aufgrund von Rissentwicklung (gezogene Linie: linear elastisches Verhalten, Rechtecke: Einfluss des spröden Zugversagens)

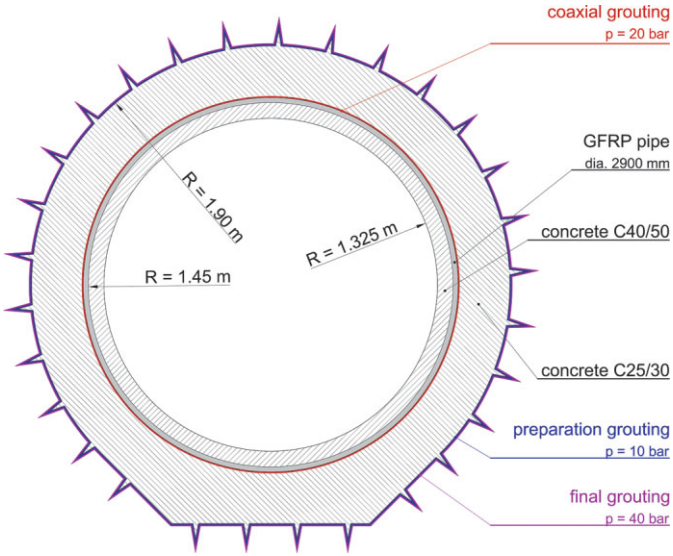

Fig. 4. Cross section of the GFRP-lined part of the tunnel
Bild 4. Regelquerschnitt des Druckstollens im Bereich der GFK-Auskleidung

wall thickness of 12.5 cm and the integrated GFRP pipe on the outer side are installed.

Every segment is 8 m long and the grouting of the contact surface between the pre-cast segment and the outer concrete shell is performed by pre-installed grouting ports. They are installed every two metres in an alternating pattern, allowing excellent control of the deformations occurring during the pre-stressing phase and granting a uniform pressure distribution. The basic layout of the regular cross section in the GFRP-lined part of the tunnel is presented in the Figure 4.

3.1 The grouting concept

In order to counter the effects of blasting damage, to ensure good bonding between the lining components and to fill the eventual discontinuities in the vicinity of the tunnel, the following grouting concept was implemented:

- Preparation grouting between the outer concrete shell and the rock mass, under the pressure of 10 bar. The intentions are the pre-stressing of the outer concrete shell, ensuring its tightness during the next stage of pre-stressing, and grouting the possibly open discontinuities in the surrounding rock mass.
- Coaxial grouting between the inner pre-cast concrete segment (with the GFRP pipe around it) and the outer concrete shell, under the pressure of 20 bar.
- Final grouting between the outer concrete shell and the rock mass, under the pressure of 40 bar. It raises the level of compressive stresses in the inner pre-cast concrete segment to its final level and induces considerable compressive stresses in the outer concrete shell as well.

4 Determination of system behaviour

4.1 Matrix stiffness method

The sandwich-type lining composed of layers of concrete, GFRP and concrete, and the interaction/superposition of the pre-stressing grout injections render the application of Seeber-diagrams inappropriate. The solution was found in the method presented by *Schwarz* [5] [6], enabling the calculation of the field quantities for an arbitrary number of concentrically placed circular layers with different material properties. It is based on assembling a stiffness matrix

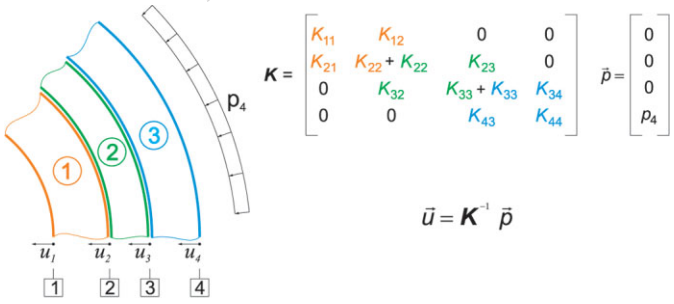

Fig. 5. The basic idea of the matrix stiffness method, when applied to the problem of concentrically joined liners with different mechanical properties
Bild 5. Die Grundidee der angewandten Deformationsmethode bei Anwendung auf konzentrisch angeordnete Auskleidungen mit unterschiedlichen mechanischen Eigenschaften

on the basis of unit deformations forced onto their respective inner and outer edges (Figure 5).

The solution of the linear equation system composed of the inverted stiffness matrix and the pressures yields the displacement of every layer edge, and thus the stresses and strains for every of them. Since a full mathematical treatise of the method is already presented in [5] [6], this work will abstain from repeating these contents and concentrate on the results.

4.2 Determination of creep and temperature losses

Creep losses have been determined on the basis of Eurocode 2 [7]. The relationships presented in the Annex B of it allow determination of creep-induced strains with incorporation of the effects of environment humidity, temperature, concrete strength, cement type, cross section geometry and concrete age. After inspecting the construction schedule, the age of both outer concrete shell and the inner pre-cast concrete shell was assumed to equal 60 days (hence assuming that both parts have been cast two months before any loads have been applied). Since the creep tendency of concrete decreases with the increasing age, this assumption delivers a certain amount of safety (the age of concrete is actually higher then 60 days, thus making the real creep-induced relaxation lower).

The initial calculations showed that the coaxial and final grouting result in relatively high compressive stresses exceeding 45 % of the compressive strength of the respective concrete layer. Therefore the creep losses have been determined by introducing increased, non-linear creep as proposed by Eurocode 2. The time interval between the respective stages of pre-stressing was assumed to equal 21 days. The results are listed in Table 1.

The shrinking of concrete was deemed irrelevant, since the shrinking strains develop in the initial stages of hydration, with a major portion of it being completed at the age of 60 days. The temperature losses have been assessed and added to the creep losses calculated for an infinite time interval. The final loss of pre-stressing due to creep and temperature decrease amounts to 60 % of the original pre-stressing level. This magnitude was deemed plausible and conservative, since the numbers stated above have been calculated with the assumption of constant loading. Since the creep magnitude is directly associ-

Table 1. Creep losses in % for both concrete types used in the lining system (numbers in brackets represent non-linear creep losses due to excessively high compressive stresses)
Tabelle 1. Kriechverluste in % für die beiden beim Ausbau eingesetzten Betonsorten (die Angaben in Klammern stehen für die nicht-linearen Kriechverluste aufgrund der überhöhten Druckspannungen)

Time [d]	Pre-cast concrete C 40/50	Outer concrete shell C25/50
60	–	–
81	16 %	20 %
102	14 (18) %	Not relevant (tension)
∞	27 (45) %	35 %

ated with the induced stresses, and the stresses decrease with the development of creep strains, the losses obtained by the assumption of constant stress magnitude represent the upper boundary of creep losses under the given circumstances.

4.3 Results

The combination of the relationships for the creep loss determination and of the matrix stiffness calculation method allowed fast determination of the resulting stress fields. A parametric study was performed, with the following design goals and constraints in mind:

- Ensuring the water tightness of the pre-cast concrete shell by preventing the development of tensile cracks;
- The compressive strength of the used materials was not to be exceeded in any pre-stressing grouting stage;
- Finding the balance between the initial pre-stressing, with the goal of enhancing the rock mass properties, and the grouting of the coaxial gap.

The solution deemed optimal features the choice of pressures of 10, 20 and 40 bar, as presented in chapter 2. The coaxial grouting was determined to be a crucial step in the pre-stressing process, due to the relatively low stiffness of the pre-cast concrete shell featuring 12.5 cm of wall thickness. The choice of grouting pressures ensured that no cracks develop in the outer concrete shell during coaxial grouting, hence preventing loss of injection liquid and granting good control of the grouting process. Simply put, a sudden loss of pressure due to a brittle tensile failure of the outer shell would induce moments in the inner shell and increase the risk of damaging it. Moreover, due to the contact stresses in coaxial gap caused by the preparation grouting, the start of coaxial grouting would become increasingly problematic with the increasing pressures of the preparation grouting (Figure 6b).

Before the contact stresses are not exceeded by the grouting pressure, no grout enters the gap and the "lift-of" of the inner shell becomes more and more sudden. In this particular case, the contact stress in the coaxial gap induced by the preparation grouting equals 0,37 MPa, meaning that the surface separation, when performing the coaxial grouting, takes place at 3,7 bar.

The final pre-stressing stage is commenced between the outer concrete shell and the ground with the grouting pressure of 40 bars. The application of a pressure in this magnitude was deemed safe because of high stiffness of outer concrete shell, making the system insensitive to non-uniform pressure distributions. The tangential stress level in the inner concrete liner is raised to its final magnitude of 31 MPa (Figure 6c).

The last load case calculated was the peak internal loading (80 bars – Figure 6d) combined with the stress distribution from the final pre-stressing with incorporated creep losses. The load-bearing capacity of the surrounding rock mass is taken into account by adding one additional term to the stiffness matrix. In order to correctly represent the stated non-linearity of the load-displacement behaviour due to creation of tensile cracks, an equivalent secant Young's modulus is calculated from the non-linear load-displacement curve. The associated maximal internal

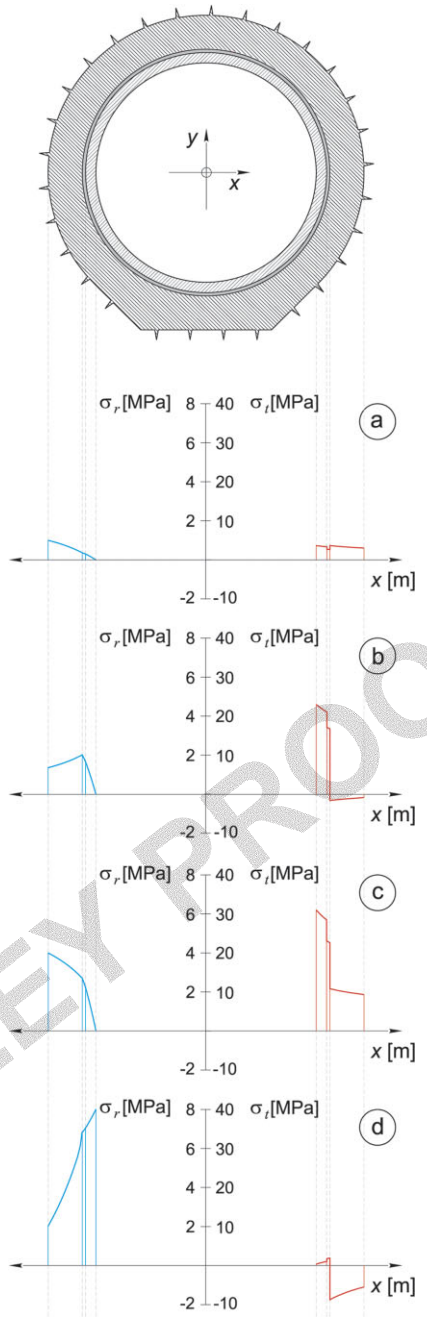

Fig. 6. The radial (blue) and tangential (red) stress distributions in the layers of the lining; a) after the preparation grouting (10 bar) has been conducted; b) after the completing the coaxial grouting (20 bar), together with the preparation grouting (creep losses included); c) the final grouting of 40 bar, together with the stress distribution from b) (creep losses included); d) stress distribution at peak load, together with the final stress distribution from c), long-term creep and temperature losses included (please note that compressive stresses are positive)
Bild 6. Die radialen (blau) und tangentialen (rot) Spannungen in den Auskleidungsschichten; a) nach der Vorinjektion (10 bar); b) nach Abschluss der Koaxialinjektion (20 bar) überlagert mit dem Spannungszustand aus der Vorinjektion (unter Berücksichtigung der Kriechverluste); c) die abschließende Vorspanninjektion (40 bar), überlagert mit dem Spannungszustand von b) (unter Berücksichtigung der Kriechverluste); d) Die Spannungsverteilung unter maximalen Innendruck, überlagert mit der Spannungsverteilung aus c), unter Berücksichtigung der Langzeit-Kriechverluste und des Temperaturabfalls (die Druckspannungen werden positiv dargestellt)

loading for the determination of the secant modulus was defined as a sum of the maximal grouts pressure (4 MPa) and the internal loading (8 MPa), hence rendering the thus obtained equivalent elastic ground properties as somewhat conservative.

The result of the calculation for this load-case confirms that no tensile stresses occur in the pre-cast concrete shell, with a probable generation of tensile cracks in the outer concrete shell. This was considered as an acceptable trade-off, since the decrease of system stiffness due to cracking of the outer shell has no significant influence on the stresses in the inner shell.

5 Determination of maximum allowable eccentricity

The findings of the calculations presented in the previous chapter brought up an additional issue: due to the considerable thickness of the outer concrete shell, the coaxial grouting has the greatest contribution to the final level of the pre-stressing. On the other hand, the relatively low wall thickness (12.5 cm) and the high level of tangential stresses induced in the lining result in a rather small margin of error, meaning that additional moments caused by uneven pre-stressing pressure distribution might result in a considerable damage to the concrete liner and unacceptable delays for the entire project. Therefore, a parametric study with the commercial numerical program ABAQUS was conducted, with the goal of determining the envelope of maximum allowable asymmetric deformations, for all stages of loading. Twenty separate calculations have been performed with the same model mesh, every calculation featuring the outer pressure p_a varying between 0 and 20 bar, raised in steps of 1 bar (Figure 7).

In every model, the liner is then additionally loaded by a point load F, causing asymmetric deformations and moments in the lining. The singular point load was used instead of other, non-uniform pressure distributions (which would depict the reality more closely) since for a known bending moment of failure, the deformations occurring in case of applied point load are minimal. This kind of load distribution represents the "worst case scenario" and lies on the safe side. The results have been evaluated by recording the minimum and maximum principal stresses at points 1, 2, 3 and 4, hence monitoring the most critical locations. The measure of asymmetric loading was defined as the difference between the radial displacements of points 1 and 3. The material was assumed to be linear elastic, and the failure has been detected by comparing the principal stresses at points mentioned above with the respective compressive and tensile strength values of the concrete. The relationship between the magnitude of the uniform pressure p_a (caused by grouting) and the maximum allowable displacement difference is hence obtained by plotting the determined displacement difference at the moment of failure (both tensile and compressive) against the pressure p_a (Figure 8).

Clearly, the maximum allowable displacement difference decreases with the increase of the grouting pressure p_a, since a smaller span between the compressive strength of concrete and the compressive stresses caused by grouting is left to be "used" by bending. Analogously, the maximum displacement difference constrained to the tensile

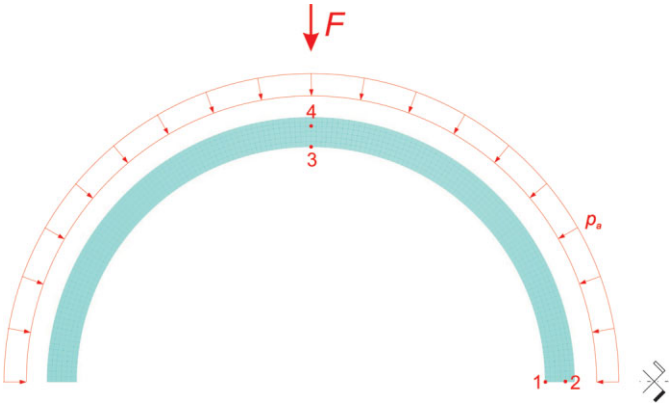

Fig. 7. Numerical model and the loads applied on it
Bild 7. Das verwendete numerische Modell und die aufgebrachten Belastungen

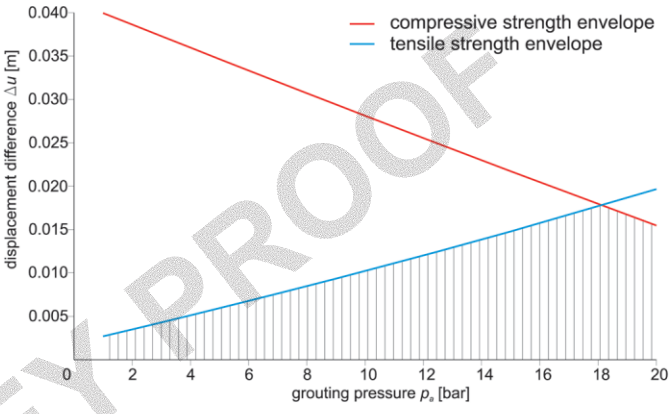

Fig. 8. The failure envelopes for both tensile and compressive failure of the pre-cast concrete lining (hatched area represents the maximum allowable displacement difference throughout the grouting pressure range)
Bild 8. Die maximalen Ovalitäten des Fertigteil-Betoninnenrohrs, ermittelt aus den Festigkeiten des Betons (der schraffierte Bereich stellt die maximale Ovalität für die gesamte Spanne des Injektionsdrucks dar)

strength of the concrete raises with the increasing grouting pressure. The area enveloped by both lines represents the allowable displacement difference under all pressure stages of coaxial grouting. Since the expected radial displacement at the end of the coaxial grouting equals approximately 1 mm, a failure caused by asymmetric loading seems to be unlikely in the light of these findings. Nevertheless, an alarm threshold of 2 mm of displacement difference was deemed reasonable, granting that no tensile cracks would develop in the initial stages of the coaxial injection.

6 Conclusion

The mathematical and mechanical background of the methods presented in this paper is well established and has been improved and combined for the application presented in this publication. It was the authors' intention to present a thorough concept for designing high pressure water tunnels, integrating state of the art in-situ testing methods, very flexible calculation method for an arbitrary number of linings, and numerical analysis into a well-

rounded design approach. Additional, more complex numerical analysis involving all of the above aspects (non-linear behaviour of the ground, concrete creep) has been conducted as well, and confirms that even in relatively deformable ground (deformation modulus equals 2,500 MPa, hence being in line with the lowest values obtained from field testing, lowest encountered overburden of 163 m and very low tensile strength of the ground) the tightness of the inner concrete shell is still ensured. The coaxial groutings will start with the beginning of September, featuring an extensive displacement monitoring programme.

The bottom line is that even challenging projects can be successfully accomplished, if all involved parties work closely together and the geotechnical investigation is extensive enough to gather the relevant design parameters, especially the (usually) unknown rock mass mechanical properties. Once they are known, the currently available calculation methods enable plausible prediction of system behaviour in almost all cases.

References

[1] *Heigerth, G., Nackler, K. and Großauer, K.*: The Feldsee pumped storage project, Felsbau 25 (2007), p. 43–51.

[2] *Seeber, G.*: Druckstollen und Druckschächte – Bemessung – Konstruktion – Ausführung. Stuttgart: Enke im Thieme Verlag, 1999.

[3] *Radoncic, N., Großauer, K., Schubert, W., Gresovnik, I. and Gober, H.-J.*: Back-analysis of elastic properties of the ground using data from a large scale plate load test. 42nd US Rock Mechanics Symposium, Paper Nr. ARMA 08-126, digital symposium proceedings. San Francisco, 2008.

[4] *Feder*, G.: Zum Stabilitätsnachweis für Hohlräume in festem Gebirge bei richtungsbetontem Primärdruck. Berg- und Hüttenmännische Monatshefte 122 (1977).

[5] *Schwarz, J.*: Druckstollen und Druckschächte – Bemessung und Konstruktion. Forschungsbericht, Lehrstuhl für Wasserbau und Wassermengenwirtschaft am Institut für Bauingenieurswesen IV. Technische Universität München, 1985.

[6] *Schwarz, J.*: Berechnung von Druckstollen – Entwicklung und Anwendung eines mathematischen Modells und Ermittlung der felsmechanischen Parameter. Dissertation, Technische Universität München, 1987.

[7] Committee CEN/TC 250 – SC: Eurocode 2 – Design of concrete structures – Part 1: General rules and rules for buildings. European Committee for Standardisation, 2005.

Dipl.-Ing. Nedim Radoncic
nedim.radoncic@tugraz.at

Dipl.-Ing. Karl Großauer
grossauer@tugraz.at

Graz University of Technology
Institute for Rock Mechanics and Tunnelling
Rechbauerstraße 12
A-8010 Graz
Austria

o.Univ.-Prof Dipl.-Ing. Dr.mont. Wulf Schubert
Schubert@tugraz.at

Dipl.-Ing. Hans-Jörg Gober
KELAG – Kärntner Elektrizitäts-Aktiengesellschaft
Arnulfplatz 2
A-9010 Klagenfurt
Austria

Em.Univ.-Prof. Dipl.-Ing. Dr.techn
Günther Heigerth
Graz University of Technology
Institute of Hydraulic Engineering and Water Resources Management
Stremayrgasse 10/II
A-8010 Graz
Austria
heigerth@tugraz.at